

---

# **sar-pre-processing Documentation**

*Release to\_be\_set*

**Thomas Weiß**

**Apr 19, 2018**

---

## Contents

---

<b>1</b>	<b>Introduction</b>	<b>1</b>
1.1	Scope . . . . .	1
1.2	Structure of this documentation . . . . .	2
<b>2</b>	<b>Installation</b>	<b>3</b>
2.1	The standard python way . . . . .	3
2.2	Using conda . . . . .	3
2.3	Using pip . . . . .	3
2.4	From code repository for developing . . . . .	3
<b>3</b>	<b>Processing Chain</b>	<b>4</b>
3.1	Overview . . . . .	4
3.2	Sentinel-1 Level-1 SLC data . . . . .	4
3.3	Precise orbit file . . . . .	6
3.4	Thermal noise removal . . . . .	6
3.5	Radiometric calibration . . . . .	7
3.6	TOPSAR Deburst . . . . .	7
3.7	Geometric correction . . . . .	8
3.8	Radiometric correction . . . . .	9
3.9	Backscatter normalisation . . . . .	9
3.10	Co-registration . . . . .	11
3.11	Multi-temporal speckle filter . . . . .	11
<b>4</b>	<b>License</b>	<b>13</b>
<b>5</b>	<b>Developers</b>	<b>14</b>
<b>6</b>	<b>version 0.4</b>	<b>15</b>
<b>7</b>	<b>version 0.3</b>	<b>16</b>
	<b>Bibliography</b>	<b>17</b>

### 1.1 Scope

D4.2 : ATBD for pre-processing: chapters on high resolution instruments [24] Algorithm Theoretical Basis Document (ATBD) for pre-processing: chapters on high resolution instruments for the processing of optical data, on Sentinel-1 pre-processing and the pre-processing of ancillary data for priors.

Need to be done !!!

Within the MULTIPLY project a new platform for joint and consistent retrieval of  
→ Copernicus SENTINEL data and beyond will be developed.

"develop a new platform for joint and consistent retrieval of Copernicus SENTINEL  
→ data and beyond" Zitat aus proposal! Zitieren?

Was written as scope for Deliverable 4.1 by Brockmann!!!!

The MULTIPLY project will "develop a new platform for joint and consistent retrieval  
→ of Copernicus  
SENTINEL data and beyond".

This document presents the Algorithm Theoretical Basis Document (ATBD) of the MULTIPLY project. The ATBD aims at providing a detailed description of the algorithms  
→ implemented in the

different processing chains, including a scientific background, a justification for  
→ each implemented

algorithm and the parameterisation used in the project.

This ATBD is written through successive increments. This initial version (v1) deals  
→ with the

coarse resolution data in general. The second version focus on the activities  
→ regarding the high-

resolution data and a last version (v3) will be released at the end of the project.  
→ The ATBD-v3 will be

the final version of the document.

## 1.2 Structure of this documentation

Need to be done !!!

This documentation gives a detailed

The documentation is organised in ... main sections.

- Section
- Section
- Section

## CHAPTER 2

---

### Installation

---

This Section will **not** be included **in** Deliverable 4.2

### 2.1 The standard python way

You can download the source code from the [project website](#). Unpack the file you obtained and then run:

```
python setup.py install
```

### 2.2 Using conda

not yet implemented

### 2.3 Using pip

not yet implemented

### 2.4 From code repository for developing

to be continued

Installation from the recent stable code repository can be done by:

```
to be continued
```

put "Sentinel-1 Level-1 SLC data" in the caption? Depends on other parts!  
How will the deliverable be organized?

### 3.1 Overview

The two Sentinel-1 satellites 1A and 1B are one of the first satellites which are providing microwave data in high temporal and spatial resolution. Within the MULTIPLY project we developed a preprocessing chain to process time-series of Sentinel-1 data for quantitative analysis of vegetation and soil parameters over agricultural fields. Therefore, rigorous geometric and radiometric corrections as well as a multi-temporal speckle filter is applied. The different preprocessing steps are shown in Fig. 3.1 and Fig. 3.2. Furthermore, every processing step is explained in more detail in the following subsections. As it can be seen Fig. 3.1 and Fig. 3.2 the preprocessing work-flow is split in two main parts. The preprocessing methods in Fig. 3.1 can be applied separately for every image. Whereas the work-flow shown in Fig. 3.2 need several images which were preprocessed by the different steps presented in Fig. 3.1.

The whole preprocessing chain for Sentinel-1 Level-1 Single Look Complex (SLC) data is accomplished by ESA's SNAP S1TBX software (current version 5.0.4). The SNAP toolbox can be downloaded from <http://step.esa.int/main/download/>. However, to automatically apply different preprocessing steps on Sentinel-1 data a python script, which uses the Graph Processing Tool (GPT) of the S1TBX, is provided. All codes, xml-graphs etc are stored in a GitHub repository accessible under <https://github.com/multiply-org/sar-pre-processing>.

### 3.2 Sentinel-1 Level-1 SLC data

The preprocessing work-flow of Fig. 3.1 is based on Sentinel-1 Level-1 SLC data. Among some other sources Sentinel-1 data can be downloaded from ESA's Copernicus Open Access Hub (<https://scihub.copernicus.eu/>).

Sentinel-1 Level-1 SLC data are generated by the operational ESA Instrument Processing Facility (IPF). The SLC products are situated in slant range geometry. The slant range geometry is the natural radar one and is defined by the line-of-sight distance of the radar system to each reflecting object. The SLC product consists of focused SAR data in zero-Doppler orientation. Furthermore, for geo-referencing orbit and attitude information directly provided

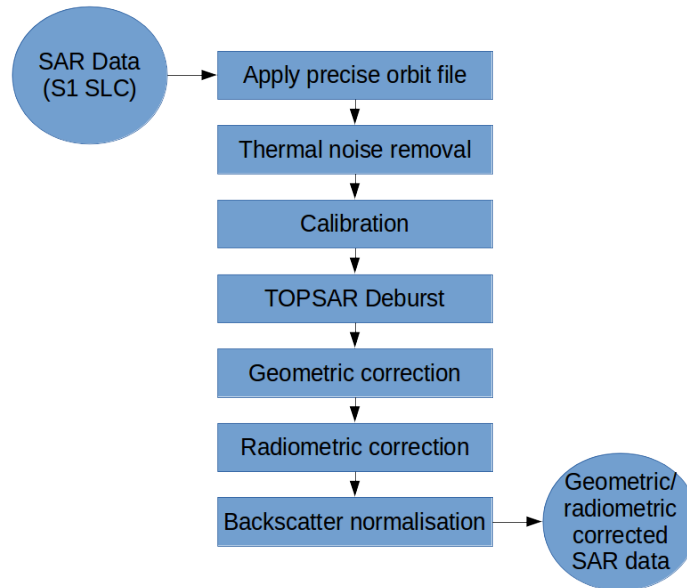


Fig. 3.1: First main part of the used preprocessing chain (rigorous geometric and radiometric correction including preliminary operations)

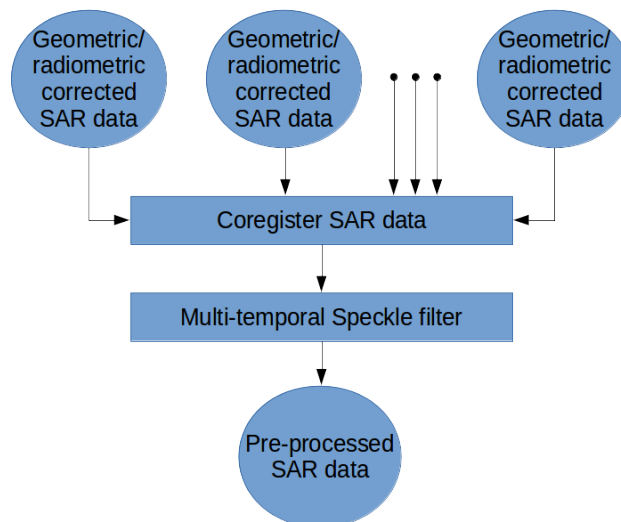


Fig. 3.2: Second main part of the used preprocessing chain (Co-registration and multi-temporal speckle filter)

by the satellite are stored within the SLC product. Moreover the SAR data is corrected for errors caused by the well known azimuth bi-static delay, elevation antenna pattern and range spreading loss [1]. In contrary to Level-1 Ground Range Detected (GRD) products SLC data preserve the real and imaginary part of the backscatter signal and contain therefore also the phase information [1]. The IPF is generating SLC data for all available acquisition modes (StripMap (SM), Interferometric Wide (IW), Extra Wide (EW), and Wave (WV)) of the Sentinel-1 satellites. Further information about Sentinel-1 Level-1 products are gathered in ESA's Sentinel-1 User Handbook [1] available at [https://earth.esa.int/documents/247904/685163/Sentinel-1\\_User\\_Handbook](https://earth.esa.int/documents/247904/685163/Sentinel-1_User_Handbook).

## 3.3 Precise orbit file

### 3.3.1 Theory / Purpose

During the acquisition of Sentinel-1 data the satellite position is recorded by a Global Navigation Satellite System (GNSS). To assure a fast delivery of Sentinel-1 products orbit information generated by an on-board navigation solution are stored within the Sentinel-1 Level-1 products. The orbit positions are later refined and made available as restituted or precise orbit files by the Copernicus Precise Orbit Determination (POD) Service. The POD products for Sentinel-1 data with given accuracy and availability after data acquisition are listed in Table 3.1.

Table 3.1: Accuracy specification for Sentinel-1 POD products [2]

Mission	POD Product	Accuracy	Latency
Sentinel-1	Restituted Orbit File	< 10 cm	3 hours
	Precise Orbit Ephemerides (POE) Orbit file	< 5 cm	20 days
	Attitude Restituted Data	< 0.005 deg	20 days

Precise orbit information can have a high influence on the quality of several preprocessing steps especially e.g. for the geo-referencing of the data. Therefore, it is always preferable to use the most accurate orbit information that is available.

### 3.3.2 Practical implementation

Since the preprocessing for the MULTIPLY project doesn't depend on near-real-time data the precise orbit file (available within 20 days) is used to update the orbit and velocity information within the Sentinel-1 SLC product. Therefore the operator "Apply Orbit Correction" of SNAP S1TBX toolbox is used.

#### Input:

- Sentinel-1 SLC IW image (downloaded from Copernicus Open Access Hub)
- Precise orbit file (automatic download by SNAP S1TBX)

#### Output:

- Sentinel-1 SLC IW image with updated orbit information

## 3.4 Thermal noise removal

### 3.4.1 Theory / Purpose

Thermal noise is caused by the background energy of a SAR receiver and independent from the received signal power. Like some other noise factors thermal noise appears randomly over the entire image. But in contrary to quantization noise like speckle, which is connected to the signal power, thermal noise is hardly noticeable. Therefore, high impact



of thermal noise on the quality of the data is especially given in areas like calm lakes, rivers and other with a low mean signal response detected by the SAR system. For the purpose of correction the IPF is calculating a thermal noise Look up Table (LUT) which is stored within the Sentinel-1 Level-1 product. More information about the calculation of the thermal noise for Sentinel-1 is given in [3].

### 3.4.2 Practical implementation

The “Thermal Noise Removal” operator of SNAP SITBX software is used to remove the thermal noise which is stored within a LUT within Sentinel-1 Level-1 products. Thermal noise removal can only applied on backscatter intensity therefore the phase information of the SLC data get lost.

**Input:**

- Sentinel-1 SLC IW image with updated orbit information

**Output:**

- Sentinel-1 SLC Intensity corrected by thermal noise

## 3.5 Radiometric calibration

### 3.5.1 Theory / Purpose

Sentinel-1 Level-1 products are not radiometric corrected by default. However, for the quantitative use of SAR images a radiometric calibration of radar reflectivity (stored as Digital Numbers (DN) within Sentinel-1 Level-1 products) to physical units (radar backscatter) is essential. Otherwise a comparison of SAR images from different sensors or even the same sensor for different acquisition dates or different acquisition modes is not possible. To apply a radiometric calibration a Calibration Annotation Data Set (CADS) with four Look Up Tables (LUTs) are provided within the Sentinel-1 Level-1 products by Sentinel-1 Instrument Processing Facility (IPF). The four LUTs are used to convert DN to sigma naught, beta naught and gamma or vice versa. More information about the radiometric calibration is given in [4].

### 3.5.2 Practical implementation

The “Radiometric Calibration” operator of SNAP SITBX software is used to perform the conversion of DN to radar backscatter. In our case the output radar backscatter information is calibrated in Sigma naught.

**Input:**

- Sentinel-1 SLC Intensity corrected by thermal noise

**Output:**

- Sigma naught calibrated radar backscatter

## 3.6 TOPSAR Deburst

### 3.6.1 Theory / Purpose

Sentinel-1 Level-1 SLC images acquired in IW or EW swath mode consists of one image per swath and polarisation. IW products are made up of three swaths which means three images for single polarisation and six images for dual polarisation. EW products are made up of five swaths which means five images for single polarisation and ten images

for dual polarisation. The sub-swath images consists of different bursts which are all processed as separate images. The different bursts are stored in one single image whereby each burst is separated by a black-filled demarcation [1]. For the usage of Sentinel-1 Level-1 SLC data only one sub-swath can be extracted or several/all sub-swath can be combined to one image with fluent transitions between the sub-swaths. More detailed information are provided in [1], [5] and [6].

### 3.6.2 Practical implementation

The “TOPSAR-Deburst” operator of SNAP S1TBX software is used to merge all sub-swath to retrieve one fluent image.

**Input:**

- Sigma naught calibrated radar backscatter (with different sub-swath)

**Output:**

- Sigma naught calibrated radar backscatter (with fluent transitions)

## 3.7 Geometric correction

### 3.7.1 Theory / Purpose

An important part of the preprocessing chain is the geometric terrain correction. The geometric correction is a conversion of the Sentinel-1 SLC data from slant range geometry into a map coordinate system. Due to the acquisition geometry of the SAR different topographical distortions like foreshortening, layover or shadowing effects occur. The appropriate way to correct these distortions is the Range-Doppler approach. The method needs information about the topography (normally provided by a Digital Elevation Model (DEM)) as well as orbit and velocity information from the satellite (stored within Sentinel-1 SLC product) to correct the mentioned distortions and derive a precise geolocation for each pixel of the image.

### 3.7.2 Practical implementation

A geometric correction of the input data is performed by using the “Range Doppler Terrain Correction” method implement in SNAP’s S1TBX software. Data from the Shuttle Radar Topography Mission (SRTM) with a resolution of 1-arc second (30 meters) is used for the necessary DEM.

**Input:**

- Sigma naught calibrated radar backscatter (with fluent transitions)
- SRTM data with 1-arc second resolution (automatic download by SNAP S1TBX)

**Output:**

- Geometric corrected sigma naught calibrated radar backscatter (Map Projection WGS84)
- Incidence angle from ellipsoid
- Local incidence angle (based on SRTM)

## 3.8 Radiometric correction

### 3.8.1 Theory / Purpose

For the conversion of Sentinel-1 backscatter values to sigma or gamma naught, LUT's stored within the Sentinel-1 product are used (see [Radiometric calibration](#)). For the creation of the LUT's Sentinel-1 IPF is using an incidence angle of an ellipsoid inflated earth model [4]. Therefore, the local terrain variation within the image and their radiometric impact on the backscatter is considered insufficiently. A simple and widely used practice to consider the radiometric impact due to local terrain variations represents the approach to use the local incidence angle instead of the ellipsoid one [7]. The radiometric corrected backscatter  $\sigma_{NORLIM}^0$  used by Kelldorfer et al. [7] can be calculated as

$$\sigma_{NORLIM}^0 = \sigma_{Ell} \frac{\sin\theta_{LIA}}{\sin\theta_{Ell}} \quad (3.1)$$

with  $\theta_{LIA}$  as the local incidence angle,  $\theta_{Ell}$  as the ellipsoid incidence angle used by IPF and the radar backscatter  $\sigma_{Ell}$  calculated by using LUT's provided by IPF.

### 3.8.2 Practical implementation

Within the “Range Doppler Terrain Correction” method of SNAP's S1TBX software the radiometric normalisation approach of Kelldorfer et al. [7] is implemented as a additional option. Unfortunately, the SNAP internal option can not be used with our kind of data. Therefore, normalisation after Kelldorfer et al [7] is done by coding the equations within the “BandMath” operator of SNAP's S1TBX. The used local incidence angle is provided by the previous applied “Range Doppler Terrain Correction” and therefore the local incidence angle is based on the SRTM data.

**Input:**

- Geometric corrected sigma naught calibrated radar backscatter (Map Projection WGS84)
- Incidence angle from ellipsoid
- Local incidence angle (based on SRTM)

**Output:**

- Radiometric and geometric corrected sigma naught calibrated radar backscatter (Map Projection WGS84)

## 3.9 Backscatter normalisation

### 3.9.1 Theory / Purpose

Beside the previously discussed geometric and radiometric distortions some other specific backscattering coefficient variations within the range direction of the image are caused by the image geometry of the SAR sensor. The backscattered energy of an illuminated area has not only a dependency on the area itself but also on the incidence angle. This means, backscatter values of a specific area with a small incidence angle return higher backscatter values then data of the same area acquired with a higher incidence angle. Incidence angle induced variations not only occur inside one image but also between images form different sensors as well as within one sensor through different acquisition geometries or different tracks or orbits. For a usage of Sentinel-1A and 1B time-series acquired with different orbits and/or different tracks and therefore most likly a high change between the incidence angles a backscatter normalisation is vital. A often and widely used technique to minimize backscatter variations caused by the incidence angle is the cosine correction [8]. The cosine correction is based on the Lambert's law for optics. Therefore, under the assumption

that the backscattered energy in the upper hemisphere follows a cosine law and also the radiation variability has a cosine dependency, the received backscatter  $\sigma_{\theta_i}^0$  and its dependency on the incidence angle can be written as

$$\sigma_{\theta_i}^0 = \sigma_0^0 \cos^n(\theta_i) \quad (3.2)$$

with a weighting factor  $n$  and the incidence angle independent backscatter  $\sigma_0^0$ . With the cosine correction the backscatter of the Sentinel-1 products can therefore normalised to a reference angle  $\theta_{ref}$  with

$$\sigma_{ref}^0 = \frac{\sigma_{\theta_i}^0 \cos^n(\theta_{ref})}{\cos^n_{\theta_i}} \quad (3.3)$$

Studies show that the weighting factor  $n$  is dependent on the roughness [9] and therefore the backscatter variations can vary with different land cover types. A schematic illustration of the backscatter variations considering the incidence angle is given in Fig. 3.3.

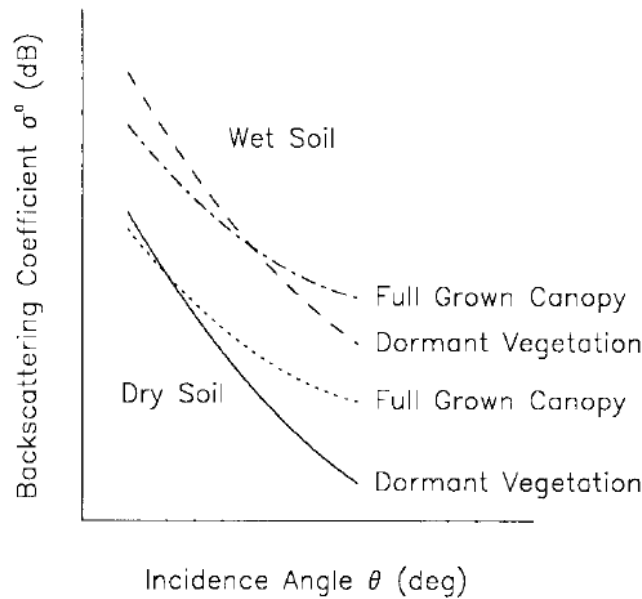


Fig. 3.3: Illustration of the backscatter variations considering the incidence angle dependency [10].

### 3.9.2 Practical implementation

The backscatter normalisation is applied by coding (3.3) in SNAP's S1TBX operator "BandMaths". As default a reference angle of 37,55° (average incidence angle for IW swath mode [3]) and a weighting factor of 2 (standard value) is specified. Through a configuration file the user can replace the default values for the reference angle and weighting factor to probably more suitable values of their specific applications.

#### Input:

- Radiometric and geometric corrected sigma naught calibrated radar backscatter (Map Projection WGS84)
- reference angle (default is 37,55°)
- weighting factor (default is 2)

#### Output:

- Radiometric and geometric corrected sigma naught calibrated radar backscatter values normalised to reference angle (Map Projection WGS84)

## 3.10 Co-registration

### 3.10.1 Theory / Purpose

For time-series analysis especially when applying a *Multi-temporal speckle filter* the SAR image has to be co-registered. The co-registration is a method to get every image of the time-series on the same grid and also the pixel resolution.

### 3.10.2 Practical implementation

The co-registration as a requirement for the *Multi-temporal speckle filter* is accomplished by the “Co-Registration” operator within SNAP’s SITBX. The “Co-Registration” operator in SNAP is defined as a completely automatic process. The operator consists of a stack creation (collocating master and slave image), a cross correlation (allignment between master and slave image) and a warp (resamples pixels from the slave image to pixels of the master image).

**Input:**

- Master image
- Slave image(s)

**Output:**

- Co-registered images

## 3.11 Multi-temporal speckle filter

### 3.11.1 Theory / Purpose

A characteristic of images acquired by a SAR system is the visibility of random noise which look like “salt and pepper” within the image and is called speckle. The appearance of speckle is caused by the interferences of coherent echoes from individual scatterers within one pixel [11]. The presence of speckle degrades the quality of the image and therefore it makes the interpretation of the SAR data more difficult. Over the years several approaches for speckle reduction were developed. They are mainly based on either multi-looking or filtering methods. Different filtering approaches like Frost, Lee etc. can be applied as a single or multi-temporal speckle filter. First findings with Sentinel-1 data show that a multi-temporal speckle filter provides better results in form of speckle reduction and resolution preservation than a single speckle filter. A major advantage for the usage of a multi-temporal speckle filter on Sentinel-1 data is the high temporal resolution availability. Nevertheless, more detailed studies on analysing the impact of different multi-temporal speckle filters on the retrieval of bio- and geophysical parameters from Sentinel-1 data are still lacking. Anyway, a usage of a multi-temporal filter significantly reduces the speckle and is therefore an essential part of our preprocessing chain.

### 3.11.2 Practical implementation

For the speckle reduction the “Multi-temporal Speckle Filter” operator within SNAP’s SITBX software is used. Currently 15 temporally consecutive images are used within the “Multi-temporal Speckle Filter” whereby the target image is temporally situated in the middle. The applied filter is a Lee filter with spatial averaging over 3x3 pixel. The spatial averaging over pixel has a significant influence on spatial resolution information loss of the image. Therefore, the averaging pixel size might change during the project. If the image consists of two polarisations the filter is applied on each polarisation separately. The practical implementation in case of filter type, used polarisation, number of used images etc. may change with more experience of applying multi-temporal speckle filters and the occurring results.

**Input:**

- 15 co-registered images

**Output:**

- speckle filtered images

**References**

## CHAPTER 4

---

License

---

to be defined
---------------

## CHAPTER 5

---

### Developers

---

- Thomas weiß <"weiss.thomas@lmu.de">



## CHAPTER 6

---

version 0.4

---

## CHAPTER 7

---

version 0.3

---

Version for presentation at MULTIPLY User Workshop in Frascati 06.02.2018

---

## Bibliography

---

- [1] Sentinel-1 Team. Sentinel-1 user handbook. Manual, ESA, Ref: GMES-S1OP-EOPG-TN-13-0001, 2013.
- [2] Sentinels POD team. Sentinels pod service file format specifications. Technical Report, ESA, Ref: GMES-GSEG-EOPG-FS-10-0075, 2016.
- [3] H. Bourbigot, H. Johnsen, and Piantanida R. Sentinel-1 product definition. Technical Report, ESA, Ref: S1-RS-MDA-53-7440, 2015.
- [4] N. Miranda and P.J. Meadows. Radiometric calibration of s-1 level-1 products generated by the s-1 ipf. Technical Report, ESA, Ref: ESA-EOPG-CSCOP-TN-0002, 2015.
- [5] D d’Aria, F De Zan, D Giudici, A Monti Guarnieri, and F Rocca. Burst-mode sars for wide-swath surveys. *Canadian Journal of Remote Sensing*, 33(1):27–38, 2007.
- [6] Francesco De Zan and AM Monti Guarnieri. Topsar: terrain observation by progressive scans. *IEEE Transactions on Geoscience and Remote Sensing*, 44(9):2352–2360, 2006.
- [7] J. M. Kellndorfer, L. E. Pierce, M. C. Dobson, and F. T. Ulaby. Toward consistent regional-to-global-scale vegetation characterization using orbital sar systems. *IEEE Transactions on Geoscience and Remote Sensing*, 36(5):1396–1411, Sep 1998. doi:10.1109/36.718844.
- [8] Fawwaz T Ulaby, Richard K Moore, and Adrian K Fung. *Microwave remote sensing: active and passive. Vol. 2, Radar remote sensing and surface scattering and emission theory*. Addison-Wesley Reading, MA, 1982.
- [9] J. P. Ardila, V. Tolpekin, and W. Bijker. Angular backscatter variation in l-band alos scansar images of tropical forest areas. *IEEE Geoscience and Remote Sensing Letters*, 7(4):821–825, Oct 2010. doi:10.1109/LGRS.2010.2048411.
- [10] W. Wagner, G. Lemoine, M. Borgeaud, and H. Rott. A study of vegetation cover effects on ers scatterometer data. *IEEE Transactions on Geoscience and Remote Sensing*, 37(2):938–948, Mar 1999. doi:10.1109/36.752212.
- [11] Iain H Woodhouse. *Introduction to microwave remote sensing*. CRC press, 2005.